Label-Free Cell Detection Using Traditional Image Processing on the LIVECell Dataset

Project Report — End Semester (ECE501: Digital Image Processing)

NetraByte — Group Members
Aashi Shah (AU2340043)   Bansi Mahkana (AU2340191)
Diya Patel (AU2340184)   Nirjara Jain (AU2340010)
School of Engineering and Applied Science (SEAS)
Ahmedabad University

Abstract—Automatic object counting seeks the accurate detection, segmentation, and quantification of multiple visually similar objects in digital images. In biomedical imaging, the task of cell counting itself is often a prerequisite for downstream analyses, such as population estimation, morphology studies, and experimental reproducibility. This report summarizes our early progress toward a cell detection and counting pipeline based on classical image processing. We outline a set of target object classes, describe the methods of contrast enhancement and noise reduction used in preprocessing, and detail further refinement using segmentation, including adaptive thresholding, edge enhancement and morphological operations. Contour extraction and connected component analysis are used to delineate and count the individual cells. Preliminary experiments conducted on a selected set of samples of the LIVECell dataset demonstrate that traditional image-processing pipelines, if properly tuned, can present promising performance in both segmentation and counting tasks, and results show competitive alignment with ground truth annotations. These results suggest the potential of classical techniques as lightweight, interpretable, and computationally efficient alternatives to deep-learning-based methods in some microscopy image analysis tasks.

Index Terms—Cell detection, segmentation, CLAHE, Connected Components, thresholding, morphological processing, contouring.

I. INTRODUCTION

Automated object detection is considered an important aspect in digital image processing, especially in biomedical applications, where cells need to be segmented and counted with high accuracy for further analysis. In this work, we intend to present the design and realization of a classical image-processing-based pipeline for performing automatic counting of cells on the LIVECell dataset: a challenging benchmark with label-free microscopy images containing diverse cell morphologies and sizes as well as various levels of overlap. The dataset contains 5,239 images with approximately 1.6 million annotated cells from eight mammalian cell lines, including A172, BV-2, BT-474, Huh7, MCF7, SH-SY5Y, SKBr3, and SK-OV-3. Specifically for this project, we have worked on the BV-2 cell line, which itself consists of 456 images. LIVECell is a challenging dataset for classic image processing due to its low contrast, overlapping, and irregularly shaped cells, along with halo artifacts inherent to phase-contrast imaging. Each image has pixel-level expert annotations, which enable the correct evaluation of segmentation performance. Our main objective was to perform appropriate cell detection in those images using only classical image processing techniques and not using deep learning models. Different from other deep learning approaches, ours depends on adaptive thresholding, morphological operations, connected component analysis, and contour extraction; therefore, this approach is preferred because it is computationally efficient and interpretable.

The goal of this project is to segment individual cells from grayscale microscopy images and then evaluate the segmented performance using standard metrics such as Accuracy, Precision, Recall, and F1-score. However, the inherent difficulty of the dataset especially non-round and overlapping cells constitutes a major problem for traditional segmentation techniques. Thus, our work in this ongoing project involves enhancing segmentation quality for round and well-separated cell types like BV2, where the performance of traditional methods is comparatively better.

Throughout the project, we refined our pre-processing and segmentation pipeline by experimenting with Gaussian blurring, tuning of adaptive thresholding, morphological noise removal, and histogram-based enhancement techniques such as CLAHE. The cell images fall broadly into two categories: distinct cells, which are more straightforward to segment due to clear separation, and clustered cells, which are in a dense packing, overlapping, and much harder to deal with. These preprocessing steps have improved boundary clarity and reduced the number of false detections, but their accuracy still remains variant based on the type of cell and the density of the overlap. On the whole, the current approach seems promising for distinct, round-shaped cells.

II. METHODOLOGY

First, we converted COCO JSON annotations into pixel-level TIFF masks in order to allow comparison with the ground truth. COCO JSON annotations present in the LIVECell dataset were converted to pixel-level TIFF masks by utilizing the pycocotools library. The final combined mask, including

cell regions as 255 and background as 0, was saved as a .tif file using OpenCV. This gives precisely the ground-truth masks required for segmentation.
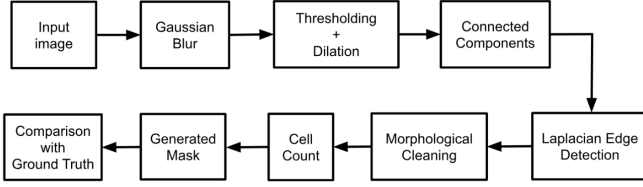
A. First approach for Scattered/Distinct Cells

Fig. 1: Flowchart for Scattered cells

1) Input Image: The original grayscale image is provided as input.

2) Gaussian Blur: The image is smoothed to reduce noise and preserve the overall structure using low-pass filter.

3) Thresholding + Dilation: The blurred image is converted into a binary mask, and dilation helps expand the cell regions and correct boundary shrinkage.

4) Connected Components: The initial cell regions are identified based on connected white pixels, meaning cells.

5) Laplacian Edge Detection: Cell edges are enhanced to highlight cell boundaries more clearly.

6) Morphological Cleaning: Additional small white noise (tiny bright spots) is removed and cell regions are recovered using morphological opening and dilation.

7) Cell Count: Each recovered cell region is counted.

8) Generated Mask: The initial cell regions are identified based on connected white pixels, meaning cells.

9) Comparision with Grount Truth: The predicted mask is compared with the provided ground truth mask to calculate accuracy and other evaluation metrics.
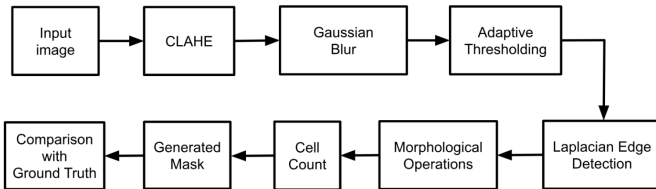
B. Second Approach for Overlapping cells

Fig. 2: Flowchart for Overlapping cells

1) Input Image: The original grayscale image is provided as input.

2) CLAHE: Contrast-Limited Adaptive Histograms Equalization (CLAHE) is applied to enhance contrast and make the cell boundaries more visible.

3) Gaussian Blur: The image is smoothed to reduce noise and preserve the overall structure using low-pass filter.

4) Adaptive Thresholding: The blurred image is converted into a binary mask; cells separated from the background.

5) Laplacian Edge Detection: Cell edges are enhanced to highlight cell boundaries more clearly using high-pass filter.

6) Morphological Operations: Operations like dilation is applied to remove noise, fill gaps, and refine the detected cell regions.

7) Cell Count: Each recovered cell region is counted.

8) Generated Mask: The initial cell regions are identified based on connected white pixels, meaning cells.

9) Comparision with Grount Truth: The predicted mask is compared with the provided ground truth mask to calculate accuracy and other evaluation metrics.
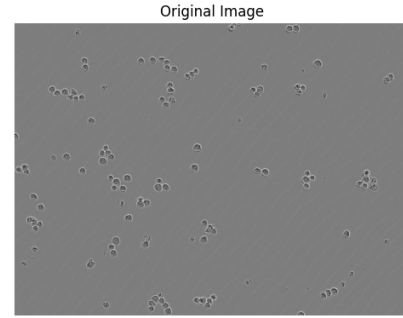
III. RESULTS AND DISCUSSION
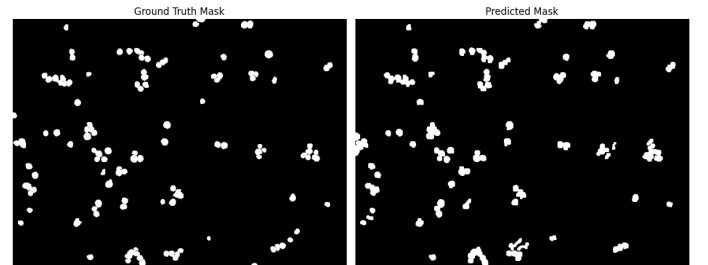

Fig. 3: First Original Image for Approach 1

Fig. 4: First Image for Approach 1

Performance Metric	Value (%)
Accuracy	98.55
Precision	79.39
Recall	89.87
F1-score	84.31

TABLE I: Performance Metrics for Fig 4
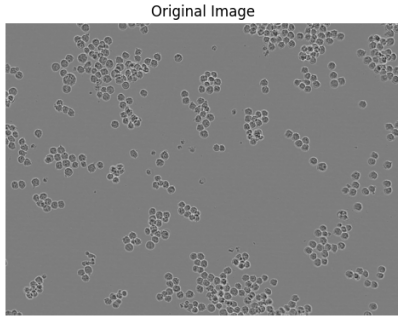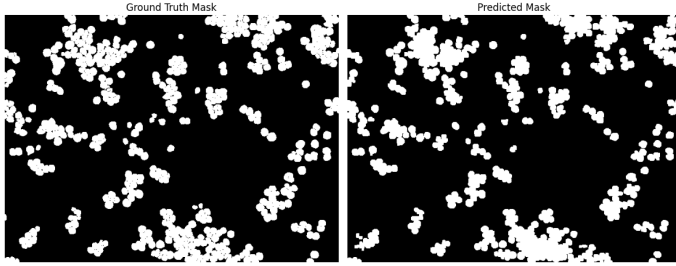
Fig. 5: Second Original Image for Approach 1

Fig. 6: Second Image for Approach 1

Performance Metric	Value (%)
Accuracy	97.17
Precision	95.25
Recall	91.27
F1-score	93.22

TABLE II: Performance Metrics for Fig 6

We observe that in both images mainly containing scattered cells, this segmentation pipeline (Approach-1) performs exceptionally well. The first image achieves 98% accuracy with an F1-score of 84%, while the second image attains 97% accuracy and an F1-score of 93%. These results indicate strong and reliable performance for scattered-cell scenarios.
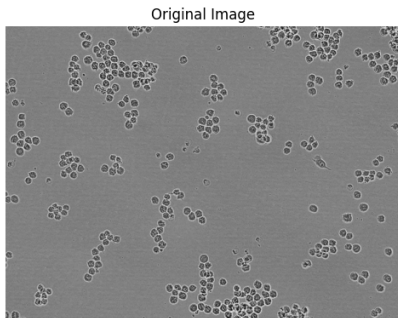

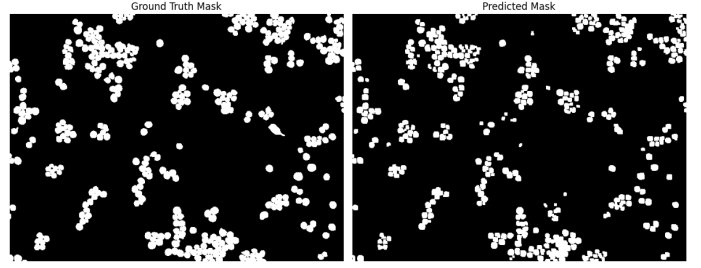Fig. 7: First Original Image for Approach 2

Fig. 8: First Image for Approach 2

Performance Metric	Value (%)
Accuracy	96.83
Precision	96.74
Recall	80.95
F1-score	88.14

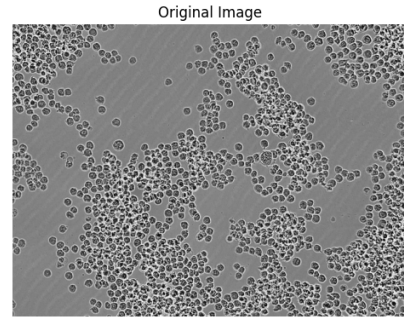TABLE III: Performance Metrics for Fig 8
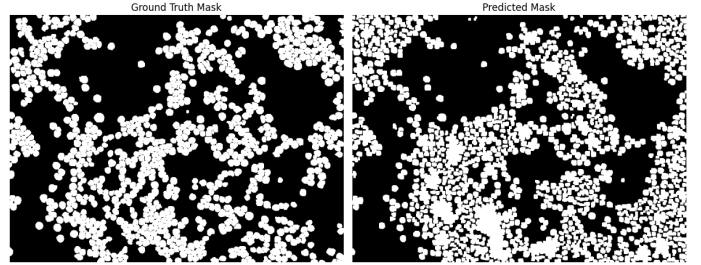

Fig. 9: Second Original Image for Approach 2

Fig. 10: Second Image for Approach 2

Performance Metric	Value (%)
Accuracy	81.01
Precision	71.59
Recall	78.90
F1-score	75.07

TABLE IV: Performance Metrics for Fig 10

We observe that in both above images, mainly containing overlapping cells, this segmentation pipeline (Approach-2) does not perform exceptionally well for all images, but it is good. The first image of this approach achieves 96% accuracy with an F1-score of 88%, while the second image attains 81%

accuracy and an F1-score of 75%. These results indicate good performance for overlapping-cell scenarios.
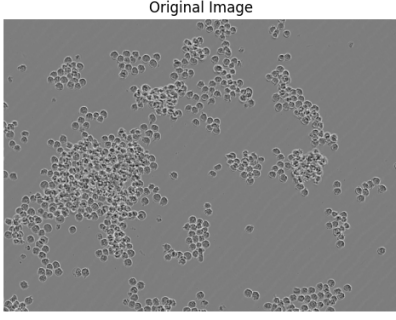

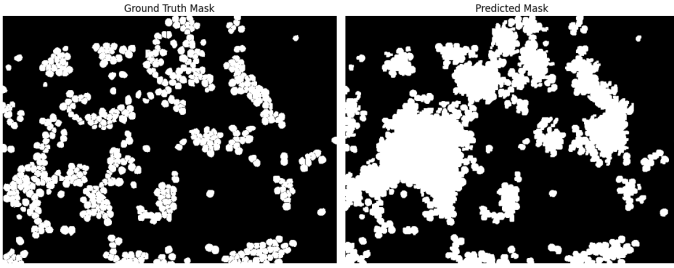Fig. 11: First Original Image for Comparison

Fig. 12: First Image for Comparison

Performance Metric	Value (%)
Accuracy	86.94
Precision	62.54
Recall	95.19
F1-score	75.49

TABLE V: Performance Metrics for Fig 12
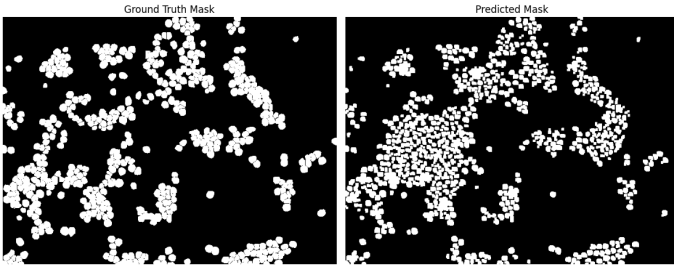
Fig. 13: Second Image for Comparison

Performance Metric	Value (%)
Accuracy	88.65
Precision	74.73
Recall	69.98
F1-score	72.27

TABLE VI: Performance Metrics for Fig 13

- A point that can be observed from our results is that many cells were not annotated in the ground truth masks

for the original images. However, Our pipeline is able to detect many of these missing cells, showing that in some instances the predicted masks could more accurately represent the actual cellular structures compared to the provided annotations. This further enhances the robustness of our approach in capturing subtle cell boundaries that might have been missed during manual labeling.

- We evaluated two different segmentation strategies to handle scattered and overlapping cells. Approach 1 performed well for scattered cells because its preprocessing phase tends to expand cell boundaries, making isolated cells easy to detect like the provided ground-truth. However, the same property caused overlapping cells to merge, leading to under-segmentation. To overcome this limitation, Approach 2 introduced a more controlled refinement that preserved boundaries among closely located cells. This resulted in very strong performance on overlapping regions compared to Approach 1, and it maintained good-though somewhat lower-accuracy but better than approach 1.

IV. CONCLUSION

This project demonstrates that, even for challenging tasks like cell detection and segmentation in phase-contrast microscopy images, an appropriately designed conventional image processing pipeline can work effectively. We achieved accurate segmentation on the LIVECell dataset's subset BV-2 by using contrast enhancement, adaptive thresholding, morphological refinement, and contour analysis without deep learning methodologies. Although there are some limitations to this work, these overall results confirm that classical techniques can still be employed for accurate, interpretable, and efficient cell segmentation.

REFERENCES

[1] C. Edlund, T. R. Jackson, N. Khalid, N. Bevan, T. Dale, A. Dengel, S. Ahmed, J. Trygg, and R. Sjögren, "LIVECell—A large-scale dataset for label-free live cell segmentation," *Nature Methods*, vol. 18, no. 9, pp. 1038–1045, 2021. [Online]. Available: https://www.nature.com/articles/s41592-021-01249-6

[2] F. Zhang, Y. Wu, M. Xu, S. Liu, C. Peng, and Z. Gao, "A morphological image segmentation algorithm for circular overlapping cells," *Intelligent Automation & Soft Computing*, Tech Science Press, vol. 32, no. 1, pp. 1–15, 2021. [Online]. Available: https://www.techscience.com/iasc/v32n1/45302/html

[3] A. Plaksyvyi, M. Skublewska-Paszkowska, and P. Powroźnik, "A comparative analysis of image segmentation using classical and deep learning approach," *Advances in Science and Technology – Research Journal*, vol. 17, no. 6, pp. 127–139, 2023. [Online]. Available: https://www.researchgate.net/publication/376127494_A_Comparative_Analysis_of_Image_Segmentation_Using_Classical_and_Deep_Learning_Approach#fullTextFileContent